NACA RM L54A07

RESEARCH MEMORANDUM

FLIGHT-DETERMINED PRESSURE MEASUREMENTS OVER THE WING OF THE DOUGLAS D-558-II RESEARCH AIRPLANE AT MACH NUMBERS UP TO 1.14

By James R. Peele

Langley Aeronautical Laboratory
Langley Field, Va.

NATIONAL ADVISORY COMMITTEE
FOR AERONAUTICS

WASHINGTON
March 12, 1954

NACA RM L54A07

NATIONAL ADVISORY COMMITTEE FOR AERONAUTICS

RESEARCH MEMORANDUM

FLIGHT-DETERMINED PRESSURE MEASUREMENTS OVER THE WING OF THE DOUGLAS D-558-II RESEARCH AIRPLANE AT MACH NUMBERS UP TO 1.14

By James R. Peele

SUMMARY

A flight investigation of the section and panel characteristics and loads obtained from pressure measurements over a 35° sweptback wing at level-flight lifts has been made through the Mach number range of 0.65 to 1.14. The section pressure distributions at the root, midspan, and tip stations varied from a subsonic type of distribution at a Mach number of 0.65 to a supersonic type of distribution at Mach numbers above 1.0.

The spanwise loading over the wing panel, which was elliptical in shape at a Mach number of 0.65 with the lateral center of pressure located at about 44 percent panel semispan, increased over the tip area near a Mach number of 1.0 with a resulting outboard shift in lateral center of pressure of approximately 5 percent. With an increase in Mach number to 1.14 the spanwise loading returned to a loading similar to that at subsonic speeds with the lateral center of pressure at about 45 percent of the panel semispan. The wing-panel chordwise center of pressure was located at 25 percent panel mean aerodynamic chord at a Mach number of 0.65 and moved forward to around 20 percent panel mean aerodynamic chord with an increase in Mach number to 0.80. At Mach numbers above 0.80 there was a rearward movement of panel chordwise center of pressure to about 44 percent panel mean aerodynamic chord at a Mach number of 1.0 followed by a forward movement of the panel chordwise center of pressure to a position of around 37 percent panel mean aerodynamic chord at a Mach number of 1.14. The theoretical relative span loading and lateral center-of-pressure location showed very good agreement with experimental data at a Mach number of 0.65.

INTRODUCTION

Swept-wing flight research data were obtained by the National Advisory Committee for Aeronautics during a series of demonstration flights of the

air-launched version of the Douglas D-558-II (rocket and turbojet) research airplane at Edwards Air Force Base, Calif. For the demonstration flights NACA instrumentation was used in obtaining data pertinent to the joint Air Force-Navy-NACA transonic flight research program.

The results of an investigation of the load distribution on the left wing panel obtained by means of pressure-distribution measurements at five span stations during rocket-turbojet powered level flights to Mach numbers of 1.14 are presented in this paper.

SYMBOLS

$b/2$ wing semispan (150 in.)

$b'/2$ spanwise distance from station 6 to wing tip (112 in.)

$C_{N'}$ wing-panel normal-force coefficient, $\int_0^1 c_n \frac{c}{\bar{c}} d\frac{2y'}{b'}$

C_{N_A} airplane normal-force coefficient, Wn/qS

$C_{m'}$ wing-panel pitching-moment coefficient about quarter-chord point of panel mean aerodynamic chord, $\frac{\bar{c}}{c'}\int_0^1 c_{m_x}\left(\frac{c}{\bar{c}}\right)^2 d\frac{2y'}{b'}$

c local wing chord, parallel to plane of symmetry unless otherwise noted

$\bar{c}$ average chord of wing panel (77.7 in.), S'/b'

c' mean aerodynamic chord of wing panel (80.44 in.),

$$2/S' \int_0^{b'/2} c^2 dy'$$

$c_{m_{c/4}}$ section pitching-moment coefficient about local quarter-chord point, $\int_0^1 -P_R\left(\frac{x}{c} - 0.25\right) d\frac{x}{c}$

[redacted]

c_{m_x} section pitching-moment coefficient about a line perpendicular to longitudinal axis of airplane, passing through quarter-chord point of mean aerodynamic chord of wing panel, $\int_0^1 -P_R\left(\frac{x}{c} + \frac{205.3 - 2.55c - 0.25c'}{c}\right) d\frac{x}{c}$

Note: Chord terms in second fraction of integrand are in inches

c_n section normal-force coefficient, $\int_0^1 P_R \, d\frac{x}{c}$

g acceleration due to gravity, ft/sec^2

M free-stream Mach number

n airplane normal acceleration, g units

P pressure coefficient, $\frac{p - p_o}{q}$

P_{cr} critical pressure coefficient; pressure coefficient corresponding to a local Mach number of 1.00

P_R resultant pressure coefficient, $\frac{p_l - p_u}{q}$

p local static pressure, lb/sq ft

p_l local static pressure on lower surface, lb/sq ft

p_o free-stream static pressure, lb/sq ft

p_u local static pressure on upper surface, lb/sq ft

q free-stream dynamic pressure, lb/sq ft

S wing area, including area projected through fuselage (175 sq ft)

S' area of wing panels outboard of station 6, the 38-inch spanwise station, (120.87 sq ft)

W airplane gross weight, lb

x distance along local chord from leading edge, ft

[redacted]

x_{cp} wing-panel chordwise center of pressure, percent c'

y spanwise distance outboard of airplane center line, ft

y' spanwise distance outboard of station 6, ft

y'_{cp} wing-panel lateral center of pressure, percent b'/2

α_A airplane angle of attack, deg

δ_{a_L} left aileron position, (positive down), deg

Subscripts:

l Conditions measured normal to 30-percent-common-chord line

AIRPLANE AND WING TEST PANEL

The Douglas D-558-II airplanes have sweptback wing and tail surfaces and were designed for Mach numbers above 1.0. Both slats and stall-control vanes or fences are incorporated on the wing of the airplane. The wing slats can be locked in the closed position or unlocked and allowed to assume a position which is a function of the angle of attack. The data presented in this paper are with the slats locked in the closed position. Photographs of the airplane are shown in figure 1 and a three-view drawing is shown in figure 2. Pertinent airplane dimensions and characteristics are listed in table I.

The profiles and ordinates of NACA 63-series airfoils presented in tables II and III are for the root and tip sections normal to the 30-percent-common-chord line, respectively. The wing test panel consists of the left wing outboard of station 6 $(2y/b = 0.256)$ and is shown in figure 3. Pressure orifices used are located at five stations on the wing test panel. Stations 6 and 7 are in a streamwise direction and stations 3 to 5 are perpendicular to the 30-percent-common chord (fig. 3). Table IV shows the measured chordwise position of the pressure orifices.

INSTRUMENTATION

Standard NACA instruments pertaining to the pressure-distribution measurements were installed in the airplane and measured the following quantities:

[redacted]

Airspeed
Altitude
Normal acceleration at center of gravity of the airplane
Airplane angle of attack and sideslip angle
Aileron and slat positions

All instruments were synchronized by means of a common timer.

An NACA high-speed pitot-static tube incorporating angle-of-attack and yaw vanes was mounted on a boom 0.95 maximum fuselage diameter forward of the nose of the airplane. The position error introduced by the pressure field in the vicinity of the tube was calibrated from $M = 0.55$ to $M = 0.80$ by the "fly-by" method and for M above 0.80 by the NACA radar phototheodolite method as presented in reference 1. The angle-of-attack values have not been corrected for position errors.

Wing-surface pressures were measured from flush-type orifices installed in the wing skin and recorded by NACA multiple-cell recording manometers. The orifices were connected by 1/8-inch inside-diameter tubing to the manometers located in the instrument compartment behind the pilot. The length of tubing varied from about 10 feet at root station to 25 feet at tip station.

TESTS AND METHODS

Wing pressure-distribution data were recorded during flights to investigate the maximum Mach number attainable with the airplane, which was accelerated from low to maximum Mach number in an altitude range of 30,000 to 40,000 feet. From these data, flight conditions were selected to determine the effects of Mach number on the wing pressure distribution. The selected data presented herein are for a $C_{N_A} \approx 0.30$ for the Mach number range of 0.65 to 0.90, $C_{N_A} \approx 0.10$ for Mach number range of 0.90 to 1.04, and $C_{N_A} \approx 0.20$ for Mach number range of 1.04 to 1.14.

Measurements of the surface pressure over the upper and lower surfaces of the wing test panel relative to the free-stream static pressure were made for stations 6 and 3 across the complete chord; at station 7, rearward of 70 percent chord, and at stations 4 and 5 forward of 10 percent chord. Differential pressure measurements were made over the rear 90 percent of the chord for stations 4 and 5.

At station 7, the chordwise pressure distributions for the first 30 percent of the chord were faired between values of individual pressure coefficients established over the first 5 percent of the chord and

values measured rearward of the 30-percent-chord point. The values of the individual pressure coefficients used over the first 5 percent of station 7 were obtained from spanwise plots of the upper- and lower-surface pressure coefficients of stations 3, 4, and 5 as shown in figure 4.

Streamwise chord loading plots were obtained from spanwise plots of the resultant pressure coefficients for stations 3, 4, and 5. A typical example is shown in figure 5. The spanwise locations of the new chordwise stations were taken at the 50-percent-chord point of the chords normal to the 30-percent common chord. The location placed the faired values at a maximum distance of 19 inches from the measured value..

Section coefficients were obtained by mechanical integration of the chordwise pressure distributions. Wing-panel coefficients were obtained by mechanical integration of spanwise distributions of loads and moments.

PRESENTATION OF DATA

Presented in figure 6 are selected pressure distributions for the upper and lower surfaces of the wing at two streamwise stations, root and tip, that show the changes in level-flight chordwise loading as the Mach number is increased from 0.65 to 1.14. Included in the figure are values of free-stream Mach number, panel normal-force coefficient, airplane angle of attack, left-aileron deflection, and critical pressure coefficient. The upper- and lower-surface pressure distributions for the midspan station, normal to the 30-percent common chord, for the same conditions as presented in figure 6 are presented in figure 7.

A summary of section pitching-moment coefficients about the 25-percent-local-chord point for the section pressure distributions presented in figures 6 and 7 is presented in figure 8.

The streamwise section load distributions for five spanwise stations presented in figure 9 are for the same conditions as presented in figures 6 and 7. Values of free-stream Mach number, airplane normal-force coefficient, integrated section normal-force coefficient, and left-aileron deflection are included for each distribution.

From the streamwise load distributions of figure 9, spanwise total load distributions and pitching-moment distributions about a line perpendicular to the longitudinal axis of the airplane passing through the 25-percent chord of the mean aerodynamic chord of the wing panel

were obtained and are presented in figure 10. Values of free-stream Mach number and panel normal-force coefficient are included.

Since the loadings in figure 10 are not at a constant panel normal-force coefficient, the relative span loading of the test panel for various Mach numbers is given in figure 11 to present a clearer picture of the wing-panel-loading variation with Mach number. Also included is the theoretical additional span loading for $M = 0.65$ obtained from reference 2.

Figure 12 presents the wing-panel chordwise and spanwise center-of-pressure variation through the Mach number range to a Mach number of 1.14. The theoretical spanwise center of pressure for $M = 0.65$ (ref. 2) is included in figure 12.

DISCUSSION

Section Characteristics

The shape of the upper-surface pressure distributions for the root, midspan, and tip stations shown in figures 6 and 7 varies from a subsonic triangular type of distribution noted at $M = 0.65$ to the rectangular distribution shown at $M = 1.14$. This change from a triangular distribution with peak negative pressures over the leading edge followed by a gradual pressure recovery over the remaining chord to a more nearly rectangular distribution causes a rearward shift in loading with increase in Mach number. The transition from the subsonic to the supersonic type of distribution is not of a smooth gradual nature because of the formation and movement of the compression shock over the upper surface. In the level-flight condition presented, one of the first indications of local shock formation is at a Mach number of 0.80 and occurs at 35 to 40 percent of the chord of the midspan station. The root station shows a very small region of supercritical flow at $M = 0.80$, but it would be difficult to try to fix the shock position below a Mach number of 0.88 because of the effect of the fuselage interference on the pressures recorded at the root station. At this Mach number the shock occurs at approximately 75-percent-chord position. The first strong indication of a shock at the tip station occurs at 35- to 40-percent-chord position at a Mach number of 0.88. With increase in Mach number the pressure distributions for all stations indicate a rearward movement of the upper-surface compression shock until the shock reaches a position of approximately 80 to 90 percent of the respective chords. These shock positions are reached at the root and midspan stations at Mach numbers of approximately 0.90 and 0.93, respectively, and seem to remain nearly stationary with further increase in Mach number. Although at a Mach number of 1.14 the shock reaches a position of about 85 percent of the chord at the tip

station, there is no indication that it will remain stationary at this position since the shock is continuing to move rearward through the limit of these tests (M = 1.14).

The pressure distribution over the lower surface presented in figures 6 and 7 shows little change for the root and midspan sections with increase in Mach number other than a gradual decrease in pressures rearward of the leading-edge region. There are no indications of any strong shocks forming on the lower surface at these two stations. However, at the tip station a compression shock forms at about 35- to 40-percent-chord position at a Mach number of 0.88. This position and Mach number are the same as were noted for the formation of the upper-surface shock, but the rearward movement of the shock on the lower surface, at Mach numbers above 0.90, precedes the shock movement on the upper surface and causes a region of down load to exist between the two shock positions.

The section pitching-moment variations through the Mach number range presented in figure 8 show an overall stable variation in section pitching moments about the section quarter-chord point at the root and midspan stations with increase in Mach number for the level-flight condition. The section pitching moment at the tip station exhibits an unstable variation with increase in Mach number to a Mach number of around 0.88, but at Mach numbers above 0.88 the variation of section pitching moment with increase in Mach number shows a stable trend as noted at the root and midspan stations. However, from root to tip there is a definite positive increase in the individual section pitching moments at all Mach numbers.

The chordwise loadings at five spanwise stations presented in figure 9 show little or no spanwise variation from a triangular type loading at a Mach number of 0.65. With increase in Mach number the loading tends to increase over the rearward portion with a corresponding decrease over the forward portion of the chords forming a more nearly rectangular or uniform type loading. This transition of the streamwise chord loadings seems to start first at the root station and progress out toward the tip. At all spanwise stations other than at the root there is a decisive reduction in chord loading behind the shock; and because the lower-surface shock precedes the upper-surface shock at the tip station, a region of down load exists. This down load is more pronounced at the tip station, diminishing as it moves inboard and rearward.

Wing-Panel Characteristics

The wing-panel load distributions shown in figure 10 indicate changes in spanwise loading occurring through the Mach number range. Inasmuch as the data of figure 10 are for level-flight conditions and are not at a constant normal-force coefficient, the changes in spanwise

loadings which occur with increase in Mach number are shown more clearly when presented as relative spanwise load distributions (fig. 11). The spanwise loading, which is elliptical in shape at a Mach number of 0.65, tends to increase over the first 60 percent of the panel semispan and to decrease over the outer portion with an increase in Mach number to a Mach number of 0.93. A further increase in Mach number brings about an increase in loading over the outer 40 percent of the panel with a decrease over the inboard 40 percent at Mach numbers near 1.0. This increased loading over the tip has disappeared at a Mach number of 1.14 with the span-load distribution again being elliptical in shape except for a slight decrease in loading over the inboard 20 percent of the wing panel.

The theoretical relative span loading and lateral center-of-pressure position for the additional air load over the wing panel at a Mach number of 0.65 obtained from reference 2 show very good agreement with the experimental data (figs. 11 and 12). The slight underestimation of the load over the outer portion of the wing panel amounts to a shift in the location of the lateral center of pressure of less than 1 percent of panel semispan.

The lateral center of pressure of the wing panel remains relatively constant at about 44 percent of the panel semispan from a Mach number of 0.65 to 0.95 as evidenced in figure 12. This result shows that the changes in span loadings noted in figures 10 and 11 for the Mach number range of 0.65 to 0.95 are not reflected in a lateral center-of-pressure movement; however, the tip loading noted previously at Mach numbers near 1.0 does result in an outboard shift of the lateral center of pressure of approximately 5 percent. Increasing the Mach number to $M = 1.14$ brings about an inboard movement of the lateral center of pressure to about 45 percent of the wing-panel semispan, which is to be expected since the panel span loading (figs. 10 and 11) has returned to a more elliptical distribution.

As stated before, since the data presented are not at constant lift, the spanwise distributions of pitching-moment coefficient shown in figure 10 do not readily indicate the stability changes encountered through the Mach number range. For these level-flight lift conditions the panel chordwise center-of-pressure movement through the Mach number range (fig. 12) indicates the changes in stability experienced by the wing panel with increasing Mach number. There is a slight decrease in wing-panel stability from a Mach number of 0.65 to 0.80 as evidenced by the forward movement of the panel chordwise center of pressure x_{cp} from a value of 25 percent of the panel mean aerodynamic chord at $M = 0.65$ to approximately 20 percent chord at $M = 0.80$. For Mach numbers above 0.80 the panel chordwise center of pressure moves rearward to about 44 percent of the panel mean aerodynamic chord at a Mach number of around 1.0 followed by a forward movement to around 37 percent of the

[redacted]

panel mean aerodynamic chord at a Mach number of 1.14. No attempt has been made to evaluate the severity of the stability reversal occurring between a Mach number of 0.92 and 0.95 since the data are at different normal-force coefficients.

CONCLUSIONS

Results of the pressure measurements over the left wing of the Douglas D-558-II research airplane during low-lift flight show that:

1. The pressure distributions at the root, midspan, and tip stations vary from a subsonic triangular type of distribution at a Mach number of 0.65 to a more nearly rectangular type of distribution at a Mach number above 1.0.

2. The panel spanwise load distribution was elliptical in shape at a Mach number of 0.65 with the lateral center of pressure occurring at about 44 percent of the panel semispan. At a Mach number of approximately 1.0 the panel loading increased over the tip area, which resulted in an outboard shift of the lateral center of pressure of approximately 5 percent; but with a further increase in Mach number to 1.14 the panel spanwise loading returned to the subsonic type of loading with the lateral center of pressure moving inboard to about 45 percent of the panel semispan.

3. The panel chordwise center of pressure was located at 25 percent of the panel mean aerodynamic chord at a Mach number of 0.65 and moved forward to approximately 20 percent chord at a Mach number of 0.80. Increasing the Mach number above 0.80 resulted in a rearward movement of the panel chordwise center of pressure to around 44 percent panel mean aerodynamic chord at a Mach number of 1.0, and at a Mach number of 1.14 the panel chordwise center of pressure moved forward to around 37 percent panel mean aerodynamic chord.

4. The relative span loading and lateral center-of-pressure location predicted by theory showed very good agreement with experimental data at a Mach number of 0.65.

Langley Aeronautical Laboratory,
National Advisory Committee for Aeronautics,
Langley Field, Va., December 22, 1953.

REFERENCES

1. Zalovcik, John A.: A Radar Method of Calibrating Airspeed Installations of Airplanes in Maneuvers at High Altitudes and at Transonic and Supersonic Speeds. NACA Rep. 985, 1950. (Supersedes NACA TN 1979.)

2. DeYoung, John: Theoretical Additional Span Loading Characteristics of Wings with Arbitrary Sweep, Aspect Ratio, and Taper Ratio. NACA TN 1491, 1947.

[redacted]

TABLE I

PHYSICAL CHARACTERISTICS OF THE DOUGLAS D-558-II AIRPLANE

Wing:	
Root airfoil section (normal to 0.30 chord of unswept panel)	NACA 63-010
Tip airfoil section (normal to 0.30 chord of unswept panel)	NACA 63_1-012
Total area, sq ft	175.0
Span, ft	25.0
Mean aerodynamic chord, in.	87.301
Root chord (parallel to plane of symmetry), in.	108.51
Tip chord (parallel to plane of symmetry), in.	61.18
Taper ratio	0.565
Aspect ratio	3.570
Sweep at 0.30 chord of unswept panel, deg	35.0
Sweep of leading edge, deg	38.8
Incidence at fuselage center line, deg	3.0
Dihedral, deg	-3.0
Geometric twist, deg	0
Total aileron area (rearward of hinge line), sq ft	9.8
Aileron travel (each), deg	±15
Total flap area, sq ft	12.58
Flap travel, deg	50
Horizontal tail:	
Root airfoil section (normal to 0.30 chord of unswept panel)	NACA 63-010
Tip airfoil section (normal to 0.30 chord of unswept panel)	NACA 63-010
Area (including fuselage), sq ft	39.9
Span, in.	143.6
Mean aerodynamic chord, in.	41.75
Root chord (parallel to plane of symmetry), in.	53.6
Tip chord (parallel to plane of symmetry), in.	26.8
Taper ratio	0.50
Aspect ratio	3.59
Sweep at 0.30 chord line of unswept panel, deg	40.0
Dihedral, deg	0
Elevator area, sq ft	9.4
Elevator travel, deg	
Up	25
Down	15
Stabilizer travel, deg	
Leading edge up	4
Leading edge down	5

[redacted]

TABLE I.- Concluded

PHYSICAL CHARACTERISTICS OF THE DOUGLAS D-558-II AIRPLANE

Vertical tail:	
Airfoil section (normal to 0.30 chord of unswept panel)	NACA 63-010
Area, sq ft	36.6
Height from fuselage center line, in.	98.0
Root chord (parallel to fuselage center line), in.	146.0
Tip chord (parallel to fuselage center line), in.	44.0
Sweep angle at 0.30 chord of unswept panel, deg	49.0
Rudder area (rearward of hinge line), sq ft	6.15
Rudder travel, deg	±25
Fuselage:	
Length, ft	42.0
Maximum diameter, in.	60.0
Fineness ratio	8.40
Speed-retarder area, sq ft	5.25
Engines:	
Turbojet	J-34-WE-40
Rocket	LR8-RM-6
Airplane weight, lb:	
Full jet and rocket fuel	15,069
Full jet fuel	11,891
No fuel	10,351
Center-of-gravity locations, percent M.A.C.:	
Full jet and rocket fuel (gear up)	22.9
Full jet fuel (gear up)	24.3
No fuel (gear up)	26.1
No fuel (gear down)	25.6

[redacted]

TABLE II

PROFILE AND ORDINATES OF ROOT SECTION
(NACA 63-010 AIRFOIL)

[Stations and ordinates given in percent of local chord]

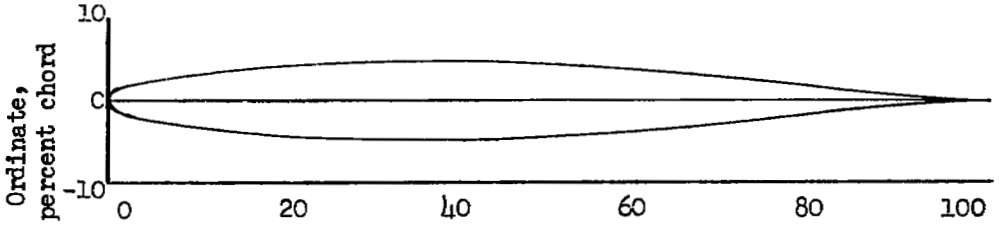

Station	Upper surface	Lower surface
0	0	0
.5	.829	-.829
.75	1.004	-1.004
1.25	1.275	-1.275
2.5	1.756	-1.756
5.0	2.440	-2.440
7.5	2.950	-2.950
10	3.362	-3.362
15	3.994	-3.994
20	4.445	-4.445
25	4.753	-4.753
30	4.938	-4.938
35	5.000	-5.000
40	4.938	-4.938
45	4.766	-4.766
50	4.496	-4.496
55	4.140	-4.140
60	3.715	-3.715
65	3.234	-3.234
70	2.712	-2.712
75	2.166	-2.166
80	1.618	-1.618
85	1.088	-1.088
90	.604	-.604
95	.214	-.214
100	0	0
L.E. radius: 0.770		

TABLE III

PROFILE AND ORDINATES OF TIP SECTION
(NACA 63_1-012 AIRFOIL)

[Stations and ordinates given in percent of local chord]

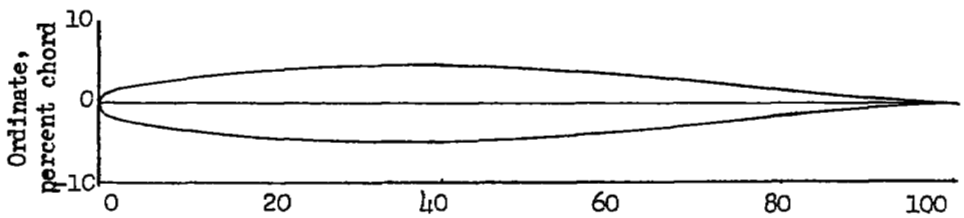

Station, percent chord

Station	Upper surface	Lower surface
0	0	0
.5	.985	-.985
.75	1.194	-1.194
1.25	1.519	-1.519
2.5	2.102	-2.102
5.0	2.925	-2.925
7.5	3.542	-3.542
10	4.039	-4.039
15	4.799	-4.799
20	5.342	-5.342
25	5.712	-5.712
30	5.930	-5.930
35	6.000	-6.000
40	5.920	-5.920
45	5.704	-5.704
50	5.370	-5.370
55	4.935	-4.935
60	4.420	-4.420
65	3.840	-3.840
70	3.210	-3.210
75	2.556	-2.556
80	1.902	-1.902
85	1.274	-1.274
90	.707	-.707
95	.250	-.250
100	0	0
L.E. radius: 1.087		

[redacted]

TABLE IV

CHORDWISE LOCATION OF PRESSURE ORIFICES

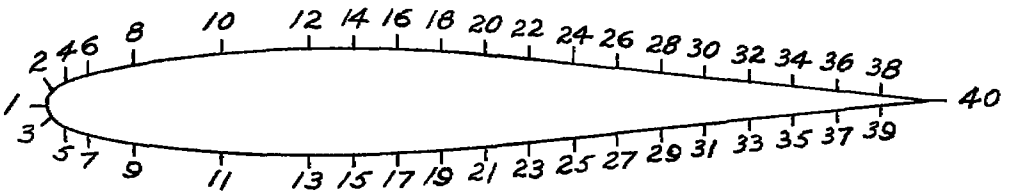

Orifice location, percent chord											
Upper surface						Lower surface					
Orifice number	Station					Orifice number	Station				
	6	8	4	5	7		6	8	4	5	7
1	0	0	0	0	- - -		- - -	- - -	- - -	- - -	- - -
2	.8	.9	1.2	.9	- - -	3	1.1	0.9	0.6	0.8	- - -
4	3.2	2.4	2.4	2.3	- - -	5	3.9	3.6	- - -	- - -	- - -
6	4.2	4.3	5.0	4.9	- - -	7	- - -	6.0	5.9	5.5	- - -
8	9.9	8.9	9.0	9.1	- - -	9	9.6	11.6	11.2	9.5	- - -
10	20.9	19.1	18.8	19.7	- - -	11	20.9	19.0	- - -	- - -	- - -
12	30.0	31.2	30.8	31.1	31.9	13	- - -	30.6	31.0	30.5	31.1
14	34.2	35.0	34.9	35.2	34.4	15	34.3	34.7	34.4	33.4	33.2
16	39.5	40.0	39.7	40.0	39.6	17	- - -	39.6	40.3	38.8	- - -
18	43.5	43.9	46.6	44.3	44.0	19	42.8	43.3	43.4	43.7	42.4
20	50.0	51.2	50.7	51.0	50.3	21	49.5	51.0	50.7	50.7	50.2
22	55.0	55.1	54.6	55.0	55.3	23	54.5	55.1	55.4	54.6	55.2
24	59.1	60.5	59.6	60.2	60.4	25	59.1	59.8	60.6	59.6	58.7
26	64.3	64.1	62.4	64.0	64.2	27	64.3	63.7	62.8	63.7	64.0
28	70.7	71.0	- - -	69.1	71.1	29	70.4	70.9	- - -	70.6	71.2
30	74.6	75.3	- - -	75.8	75.1	31	74.4	75.5	- - -	76.3	75.2
32	78.0	80.2	- - -	79.8	83.3	33	77.7	80.2	- - -	79.4	79.4
34	84.7	84.9	84.7	85.7	85.9	35	84.4	85.2	85.6	85.5	85.9
36	90.2	90.0	89.8	89.5	90.0	37	90.0	90.3	89.6	89.2	89.8
38	95.1	94.6	94.2	95.0	95.0	39	94.3	94.4	95.2	94.9	95.0
40	- - -	- - -	97.7	98.6	98.4	40	98.3	98.8	- - -	- - -	- - -

[redacted]

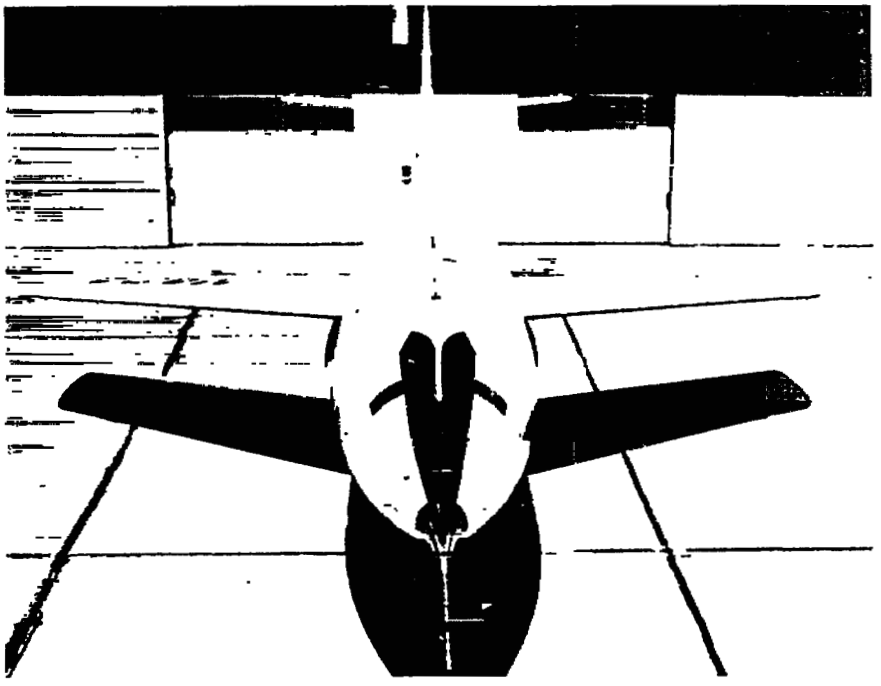

(a) Front overhead view.

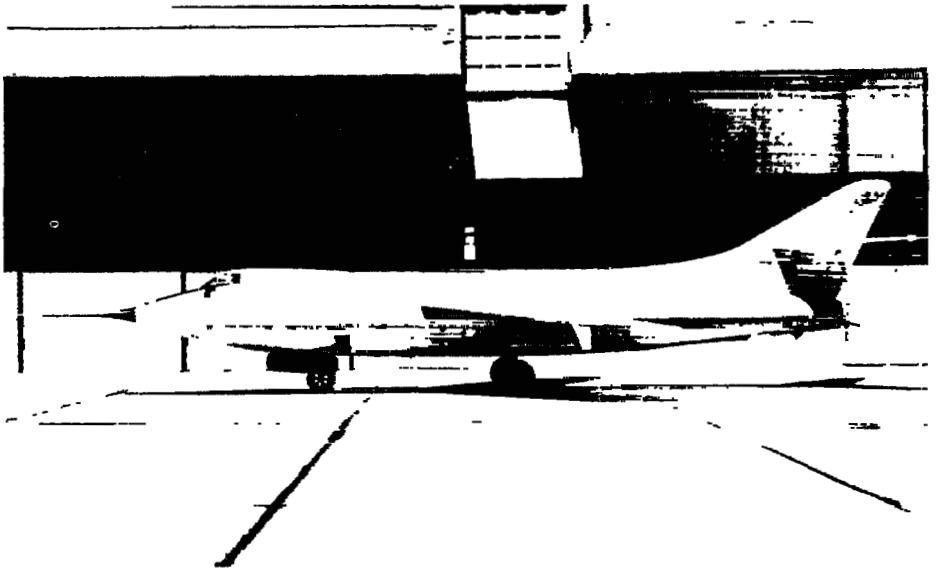

L-82072

(b) Side view.

Figure 1.- Photographs of the Douglas D-558-II research airplane.

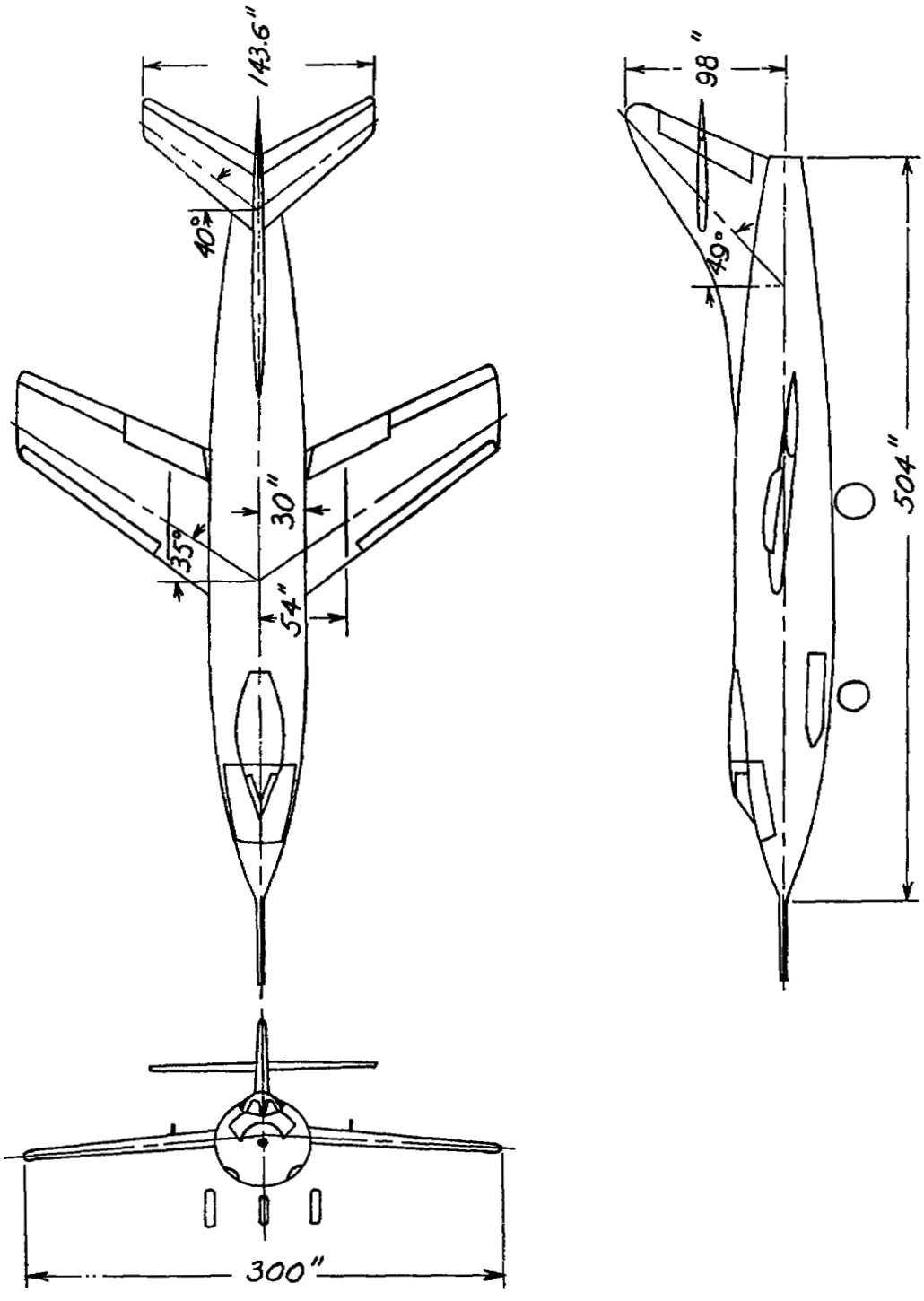

Figure 2.- Three-view drawing of Douglas D-558-II airplane.

[redacted]

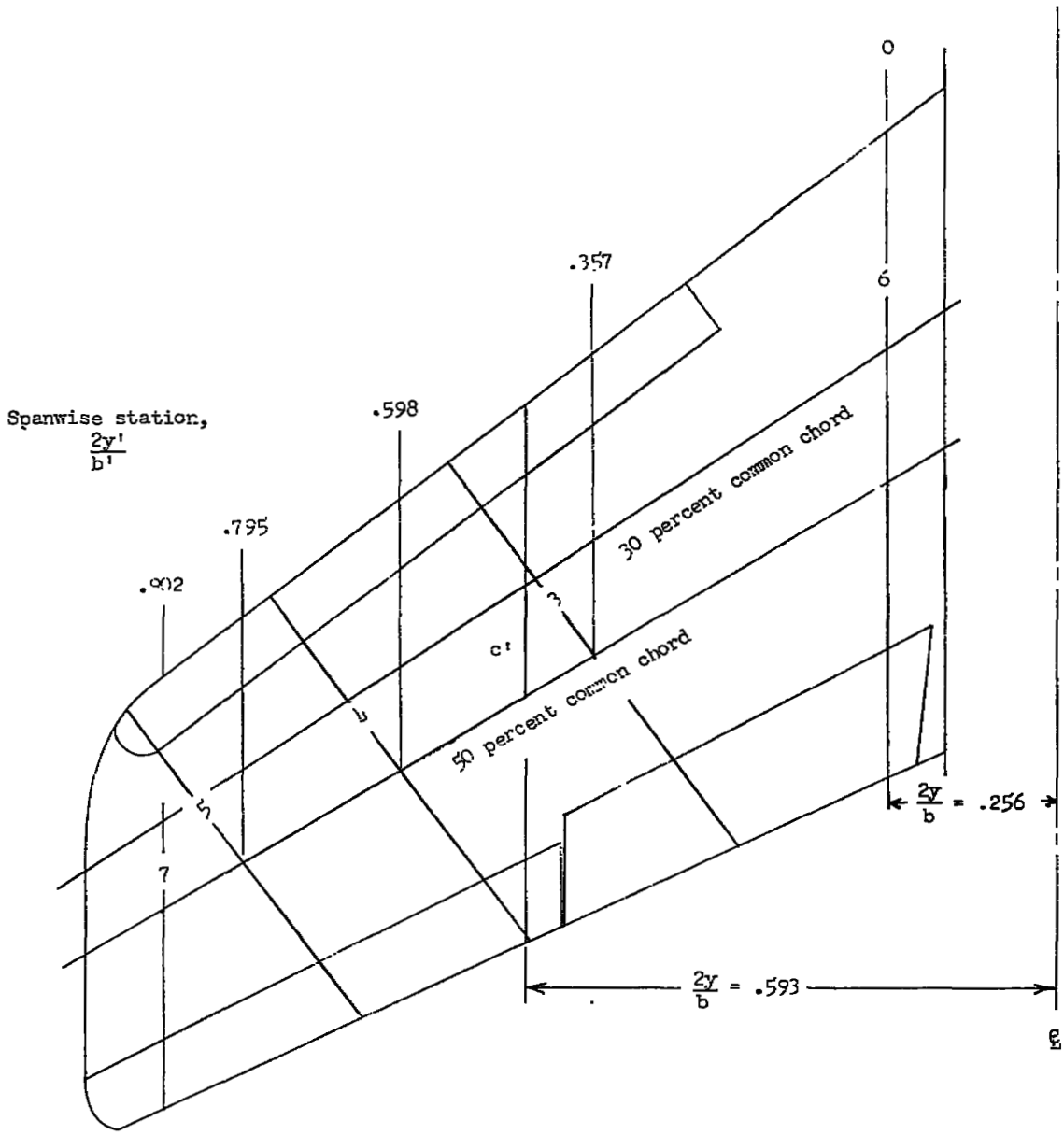

Figure 3.- Location of pressure-orifice stations.

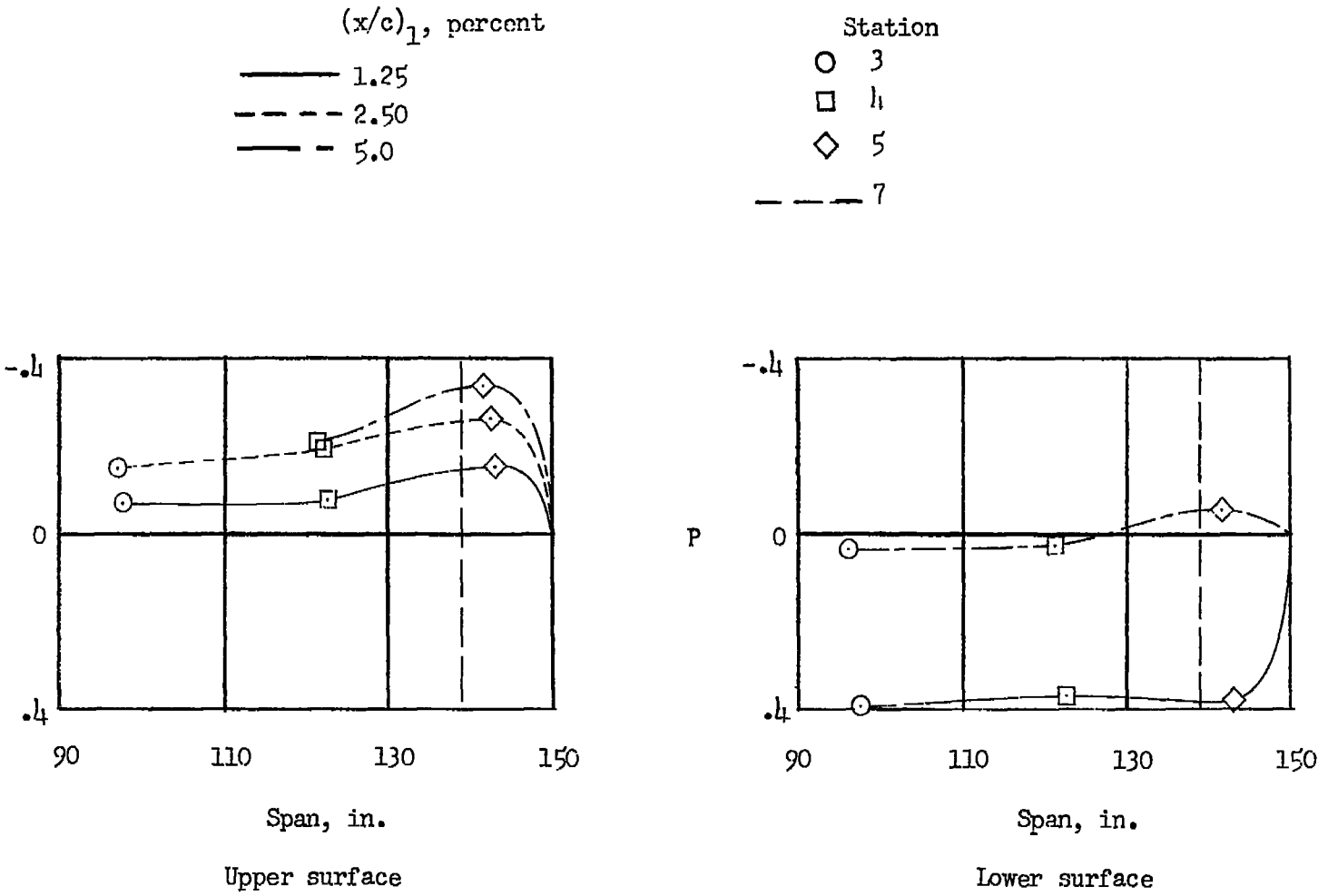

Figure 4.- Example of spanwise plot of individual pressure coefficients over leading edge of wing tip.

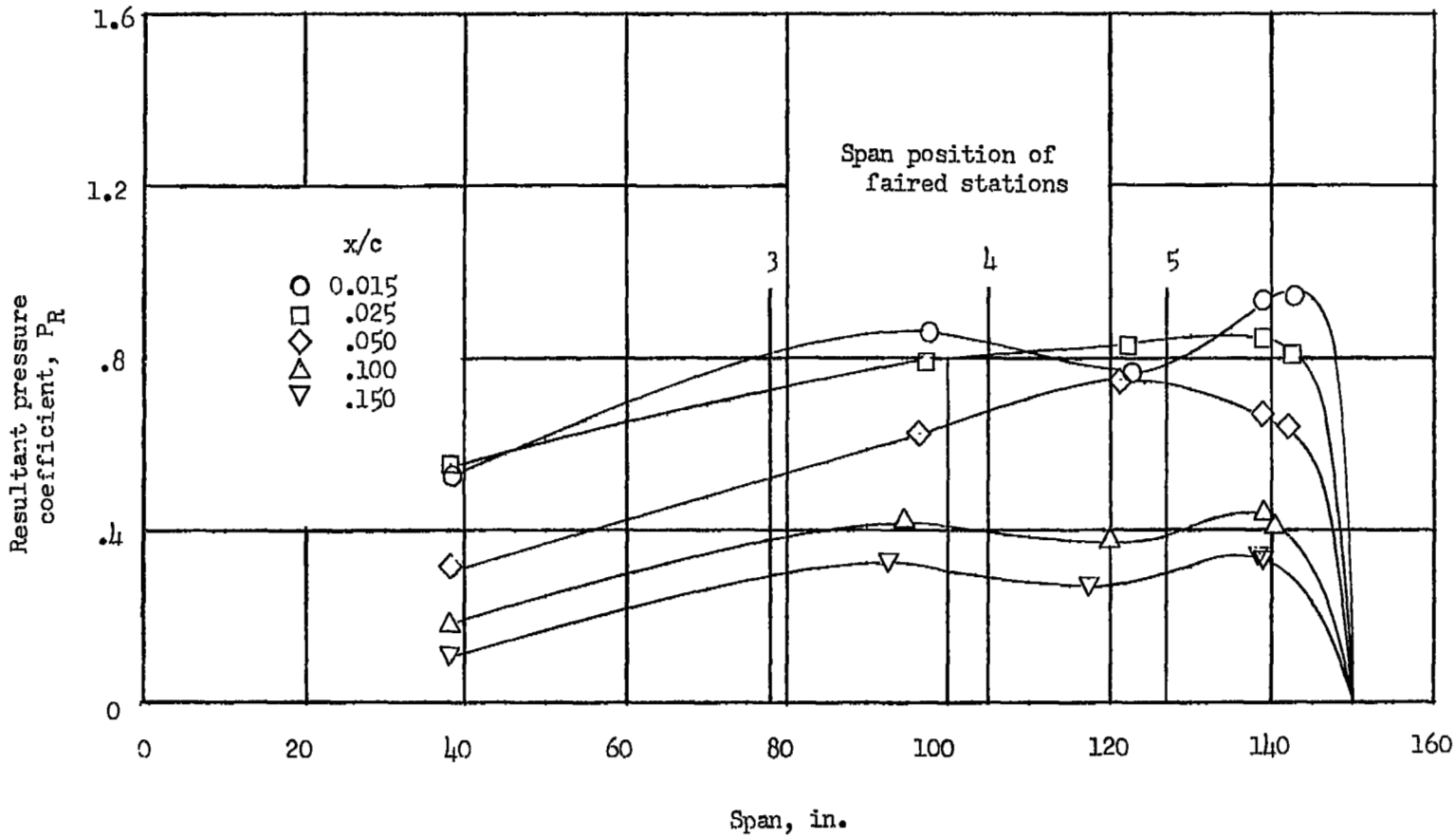

Figure 5.- Typical spanwise plot of resultant pressure coefficients over the wing panel.

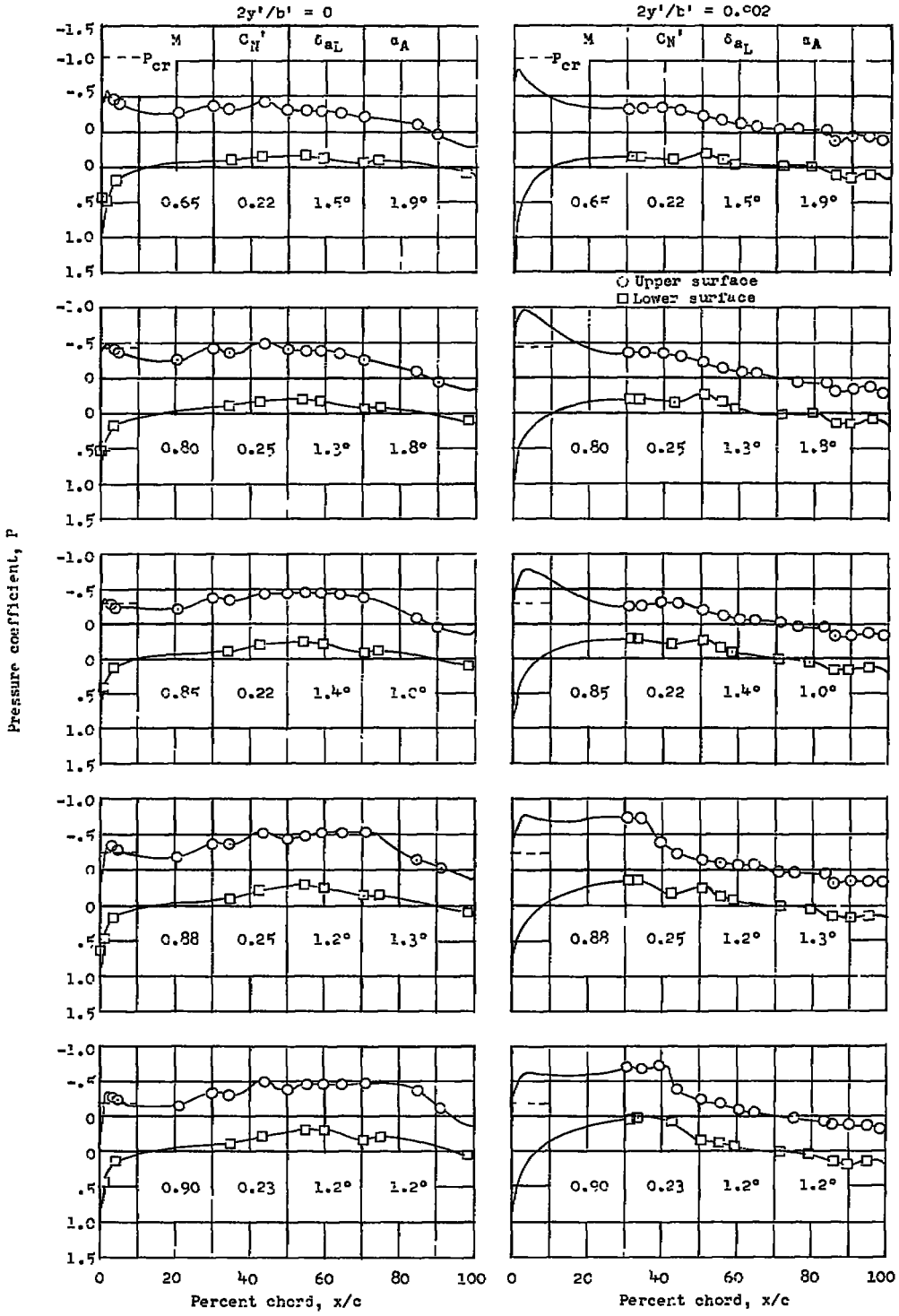

Figure 6.- Chordwise pressure distribution at root and tip stations.

[redacted]

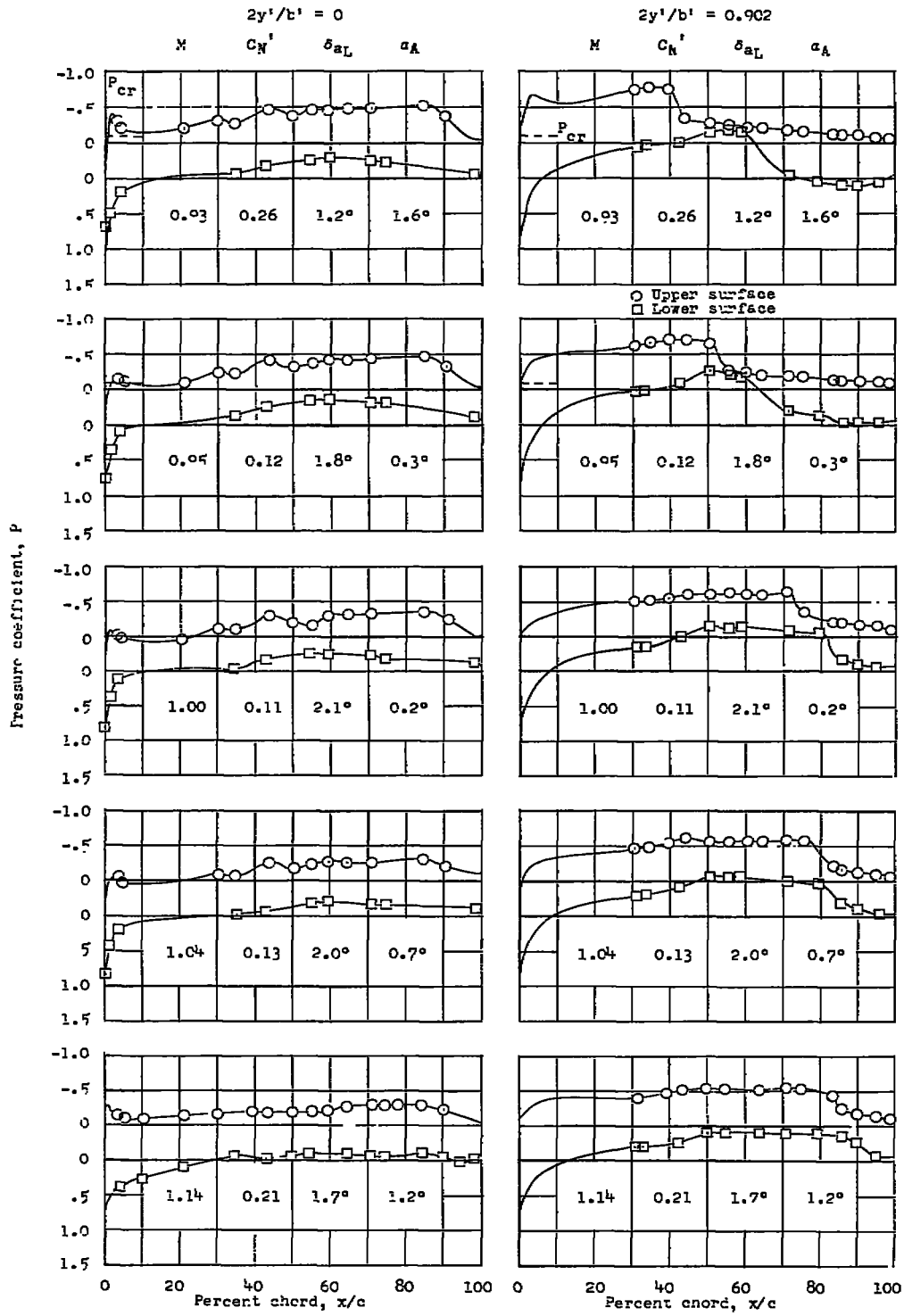

Figure 6.- Concluded.

[redacted]

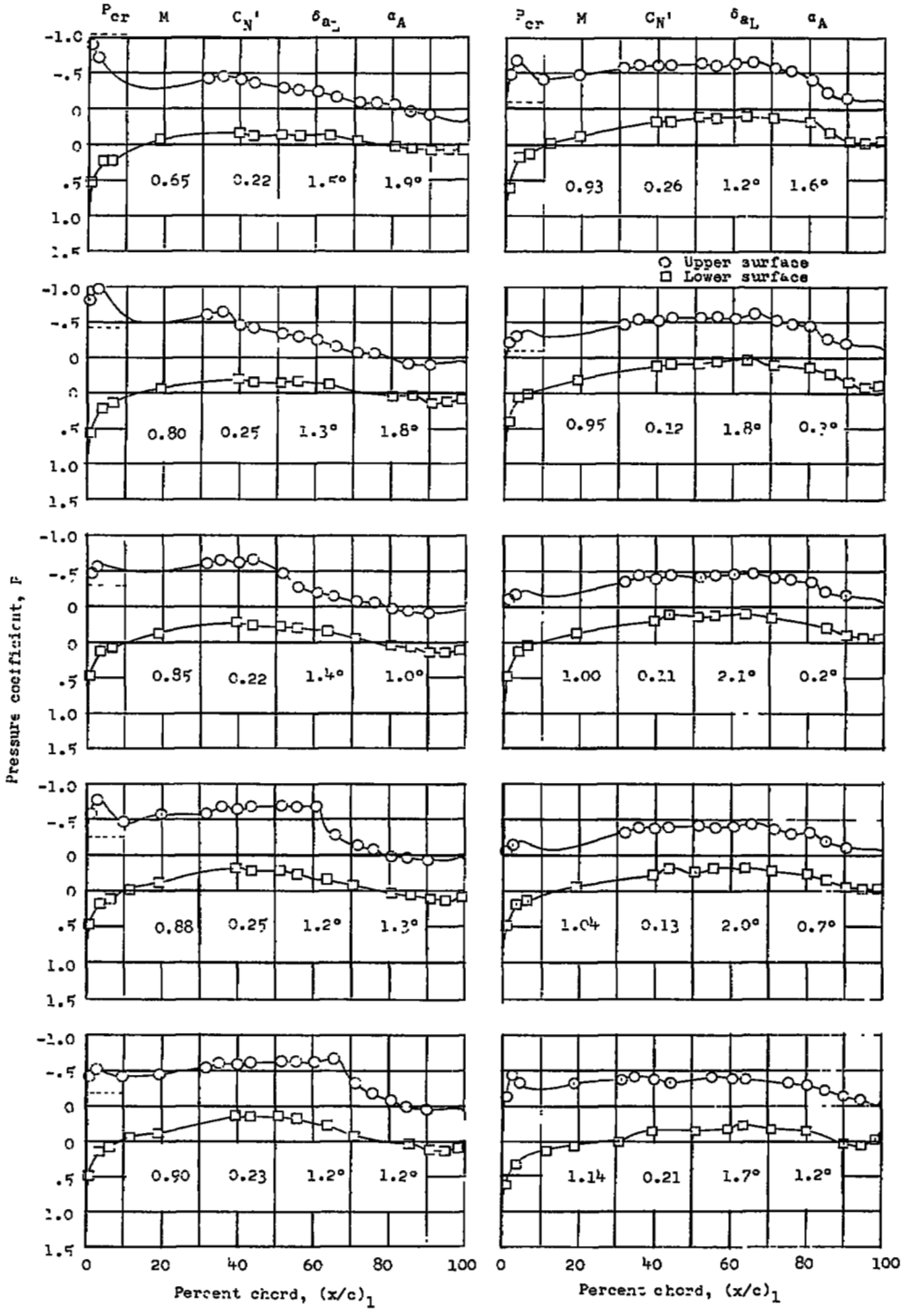

Figure 7.- Chordwise pressure distribution at midspan station located normal to 30-percent-common chord line.

[redacted]

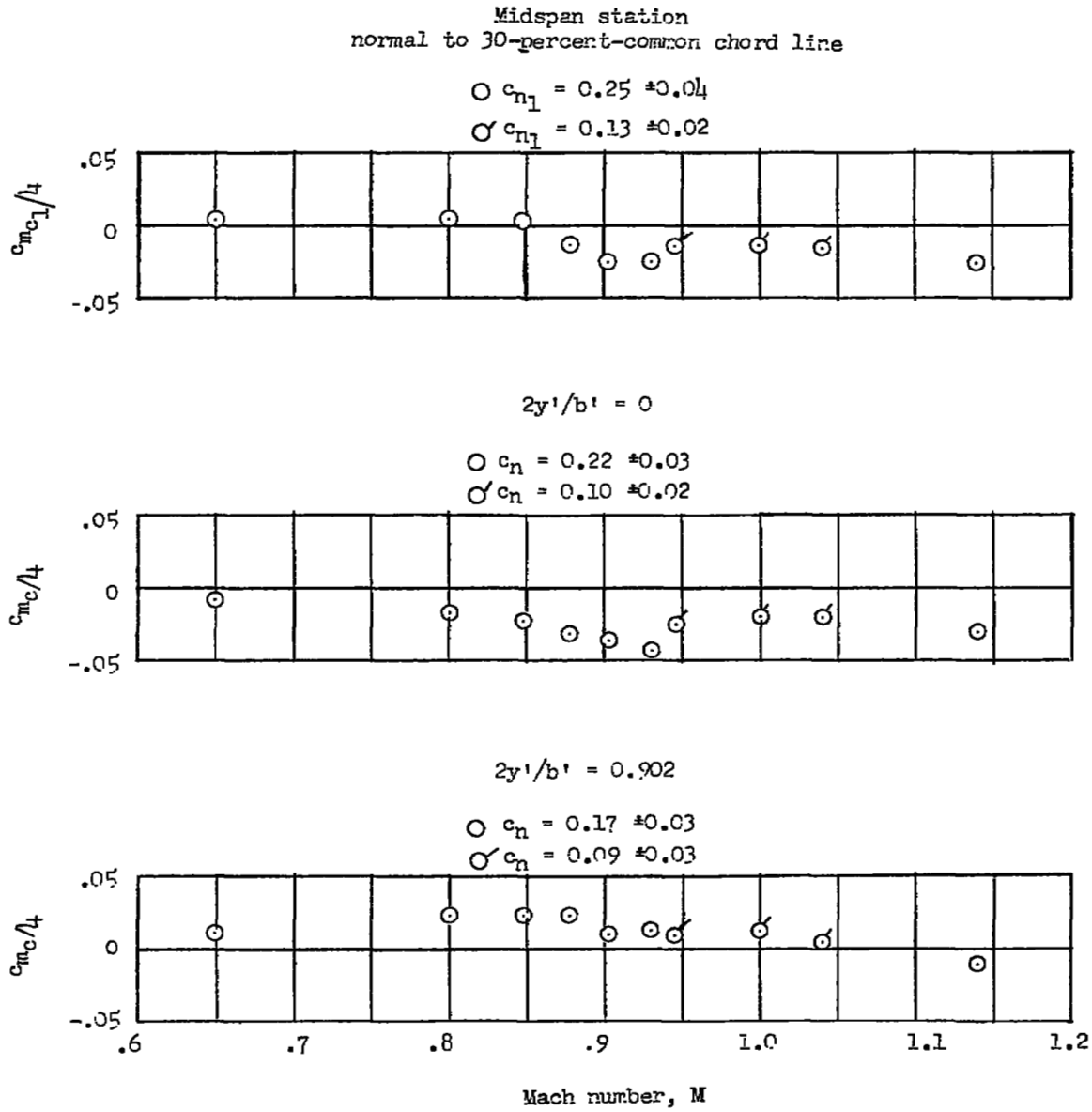

Figure 8.- Variation of the section pitching-moment coefficient with Mach number.

[redacted]

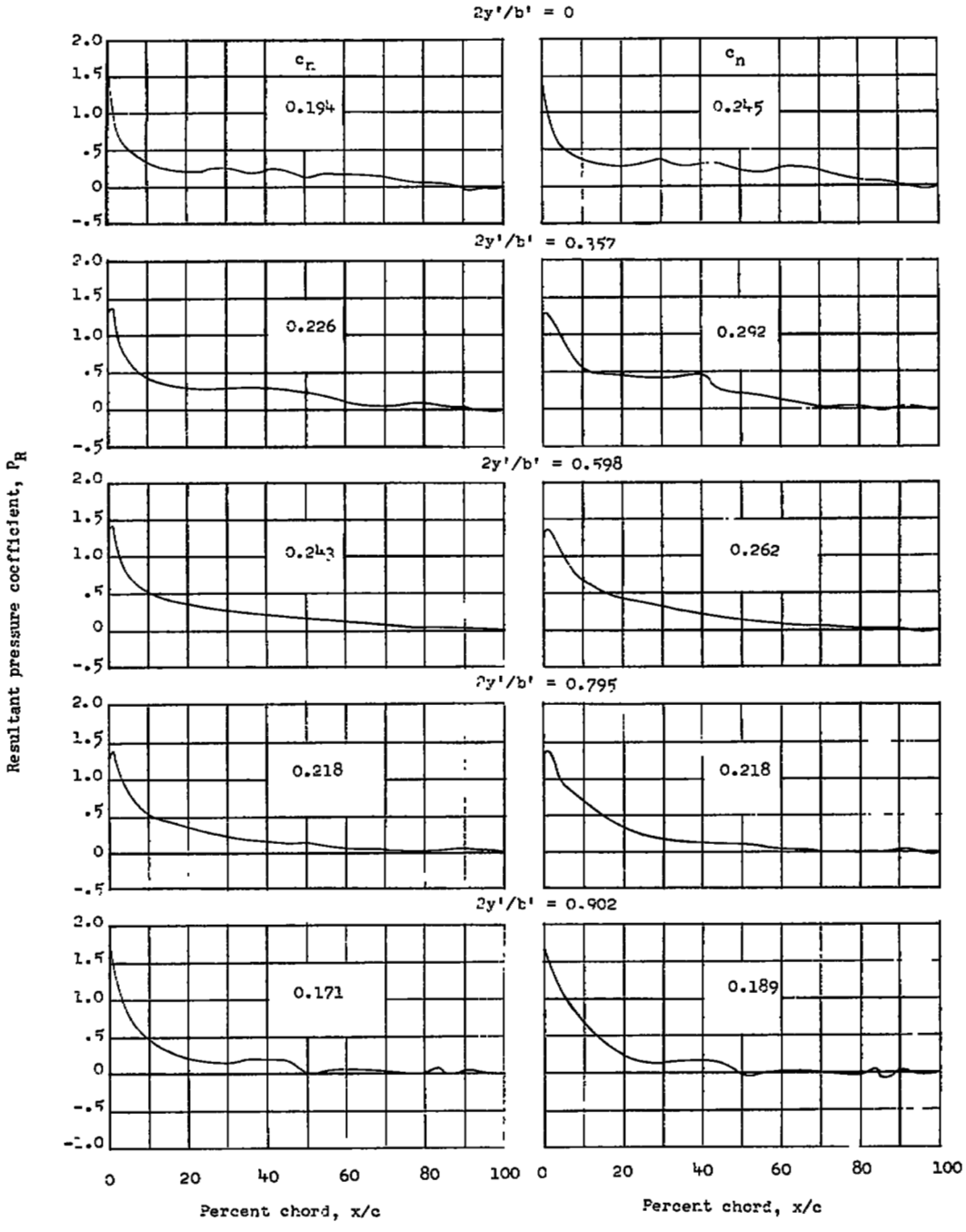

(a) $M = 0.65$; $C_{N_A} = 0.23$; $\delta_{a_L} = 1.5^\circ$.

(b) $M = 0.80$; $C_{N_A} = 0.25$; $\delta_{a_L} = 1.3^\circ$.

Figure 9.- Chordwise load distribution over the wing panel.

[redacted]

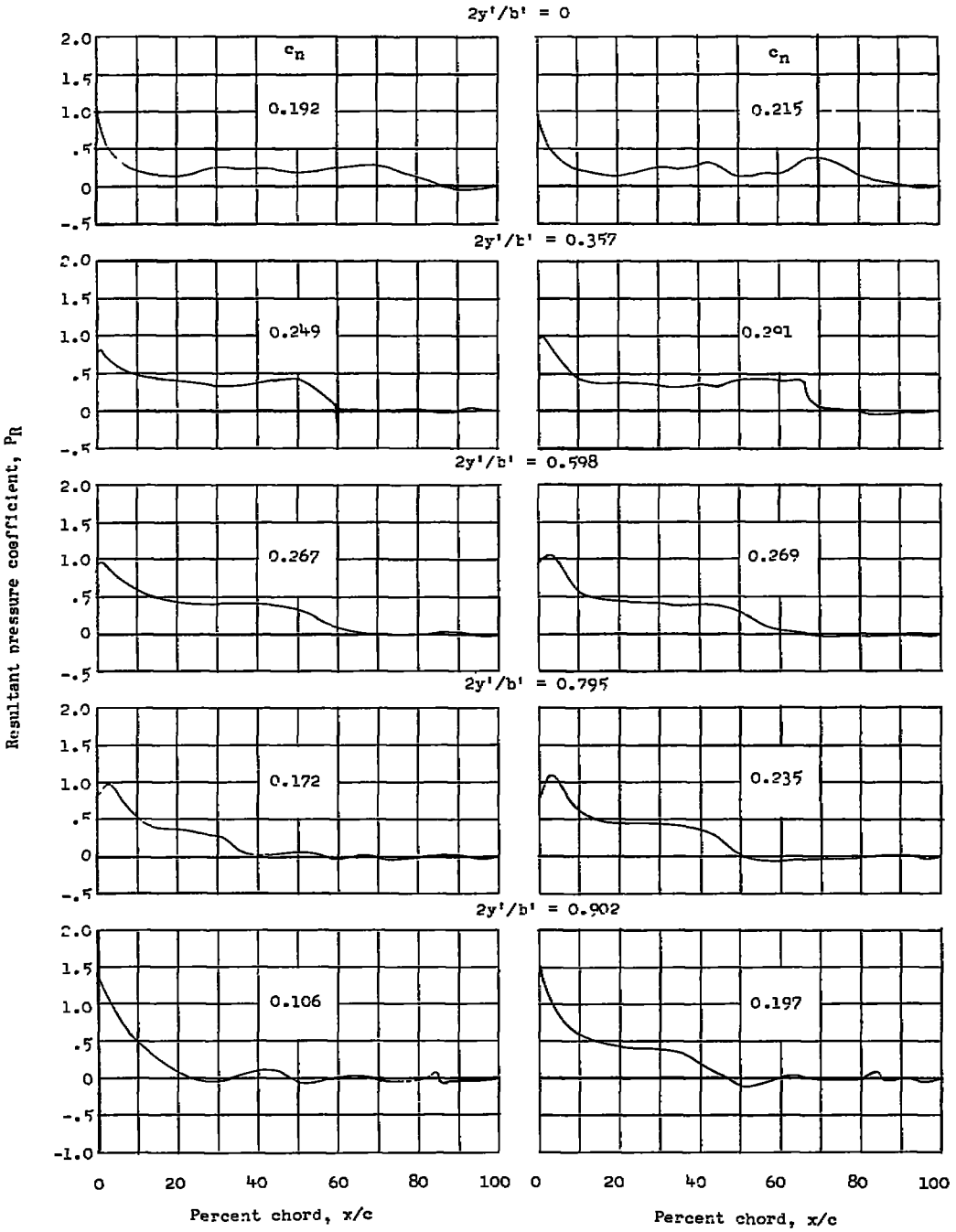

(c) $M = 0.85$; $C_{N_A} = 0.19$; $\delta_{a_L} = 1.4°$.

(d) $M = 0.88$; $C_{N_A} = 0.25$; $\delta_{a_L} = 1.2°$.

Figure 9.- Continued.

[redacted]

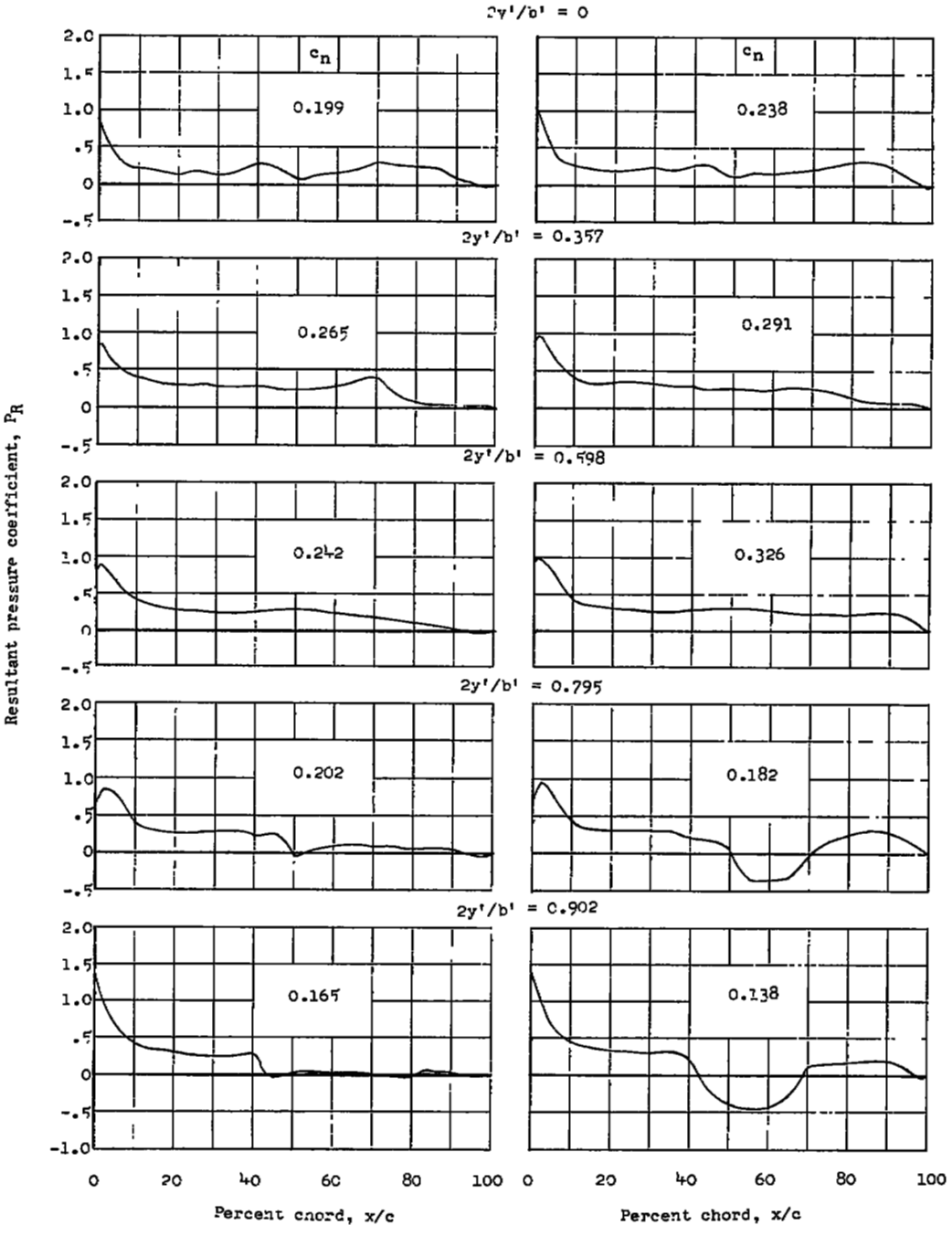

(e) M = 0.90; C_{N_A} = 0.22; δ_{a_L} = 1.2°.

(f) M = 0.93; C_{N_A} = 0.23; δ_{a_L} = 1.2°.

Figure 9.- Continued.

[redacted]

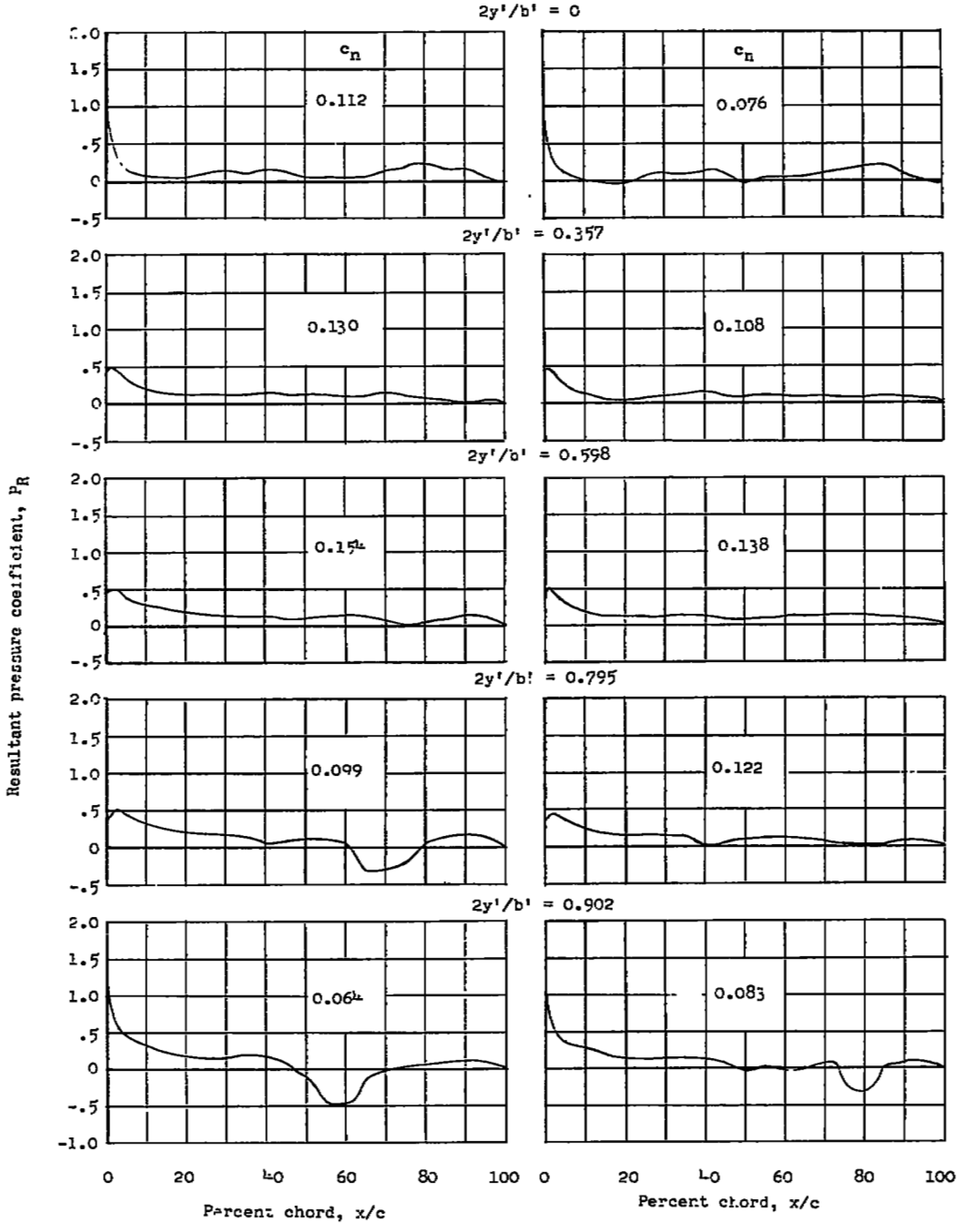

(g) $M = 0.95$; $C_{N_A} = 0.13$; $\delta_{a_L} = 1.8^\circ$.

(h) $M = 1.00$; $C_{N_A} = 0.10$; $\delta_{a_L} = 2.1^\circ$.

Figure 9.- Continued.

[redacted]

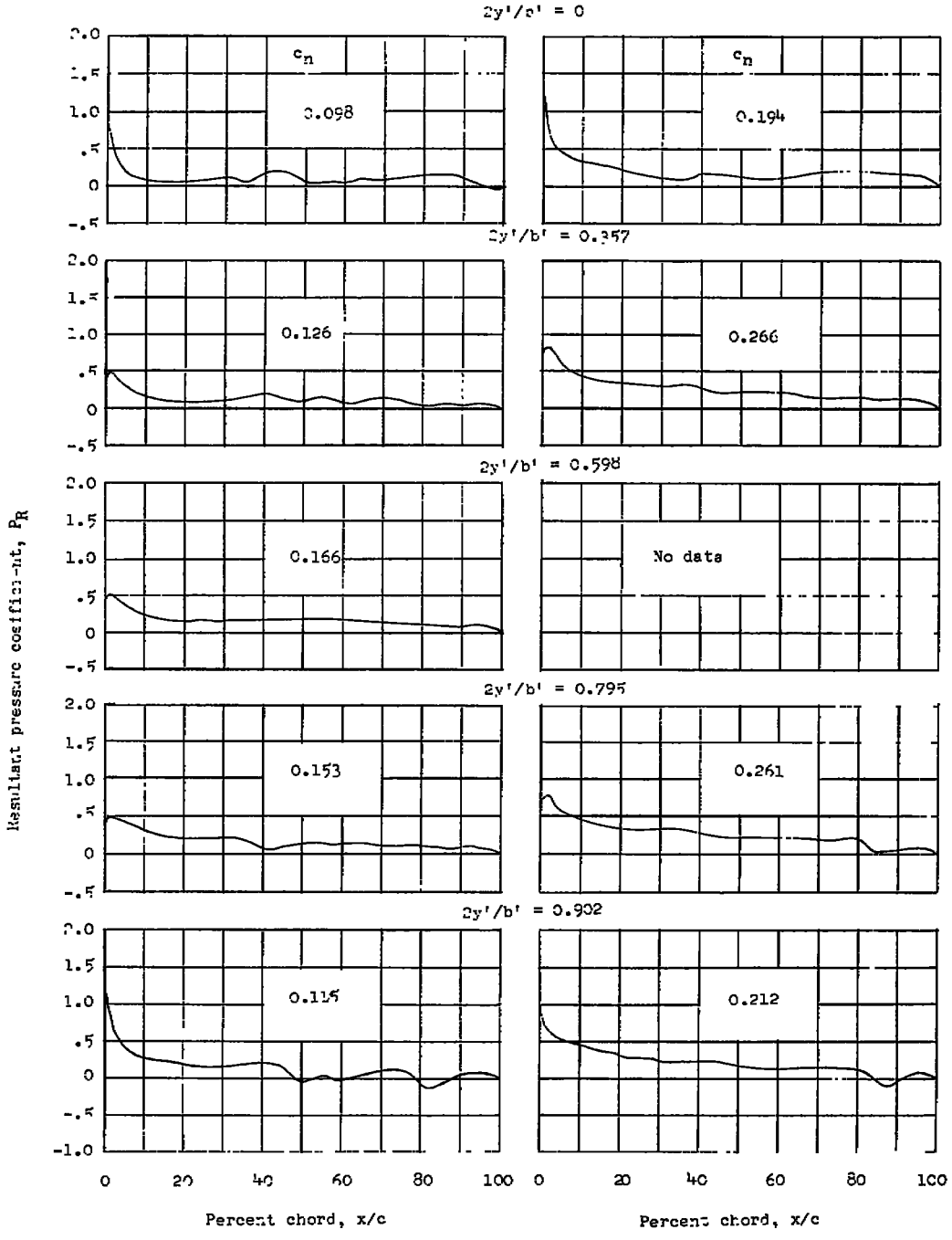

(i) M = 1.04; C_{N_A} = 0.12; δ_{a_L} = 2.0°.

(j) M = 1.14; C_{N_A} = 0.21; δ_{a_L} = 1.7°.

Figure 9.- Concluded.

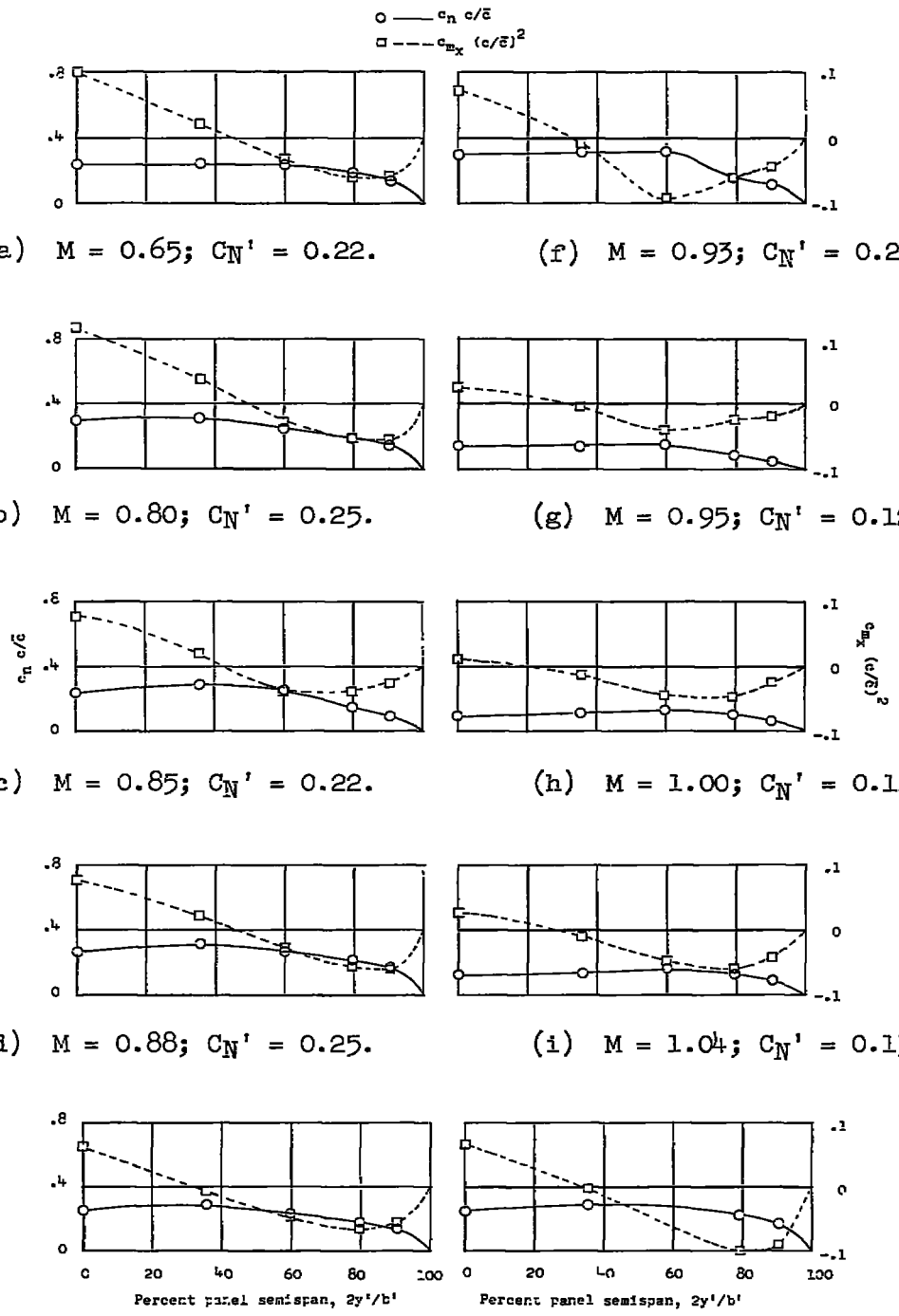

(a) M = 0.65; C_N' = 0.22.

(b) M = 0.80; C_N' = 0.25.

(c) M = 0.85; C_N' = 0.22.

(d) M = 0.88; C_N' = 0.25.

(e) M = 0.90; C_N' = 0.23.

(f) M = 0.93; C_N' = 0.26.

(g) M = 0.95; C_N' = 0.12.

(h) M = 1.00; C_N' = 0.11.

(i) M = 1.04; C_N' = 0.13.

(j) M = 1.14; C_N' = 0.25.

Figure 10.- Span load and pitching-moment distributions over the wing panel.

[redacted]

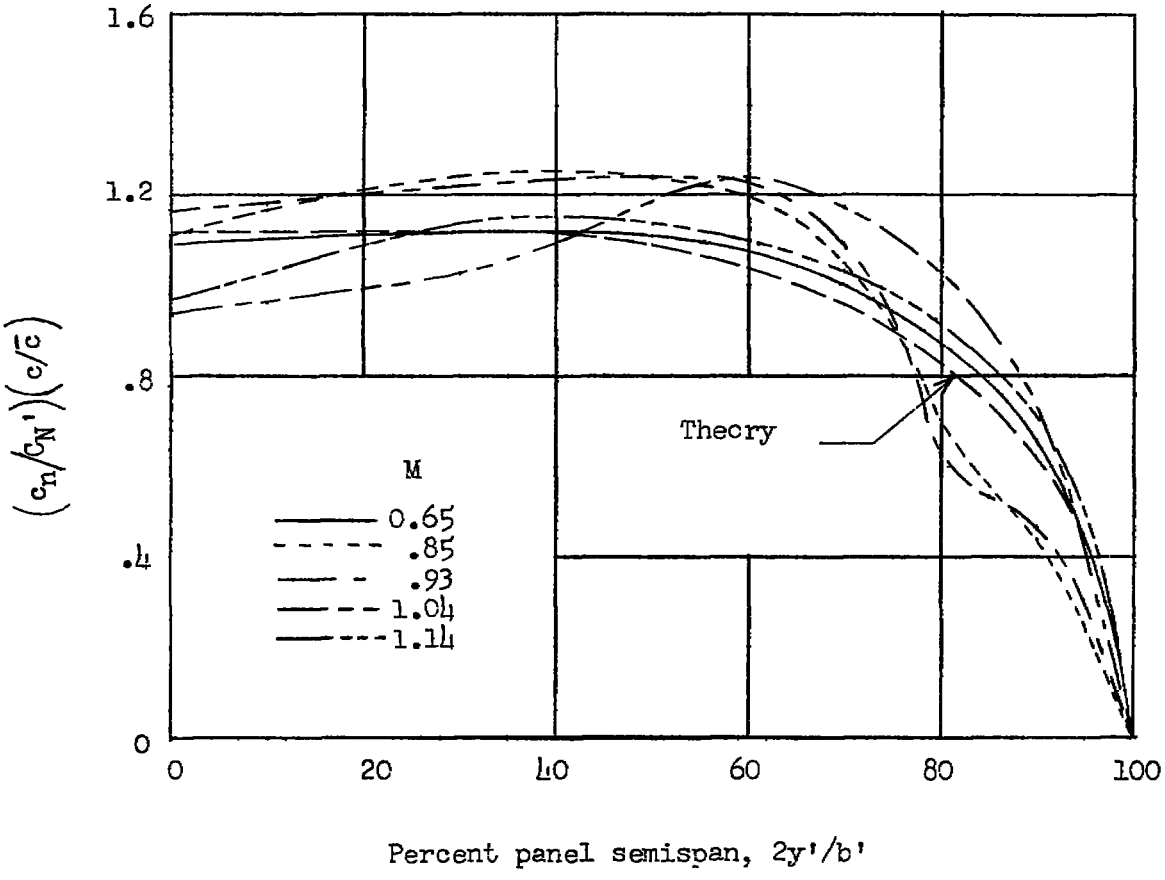

Figure 11.- Relative span loading of wing panel.

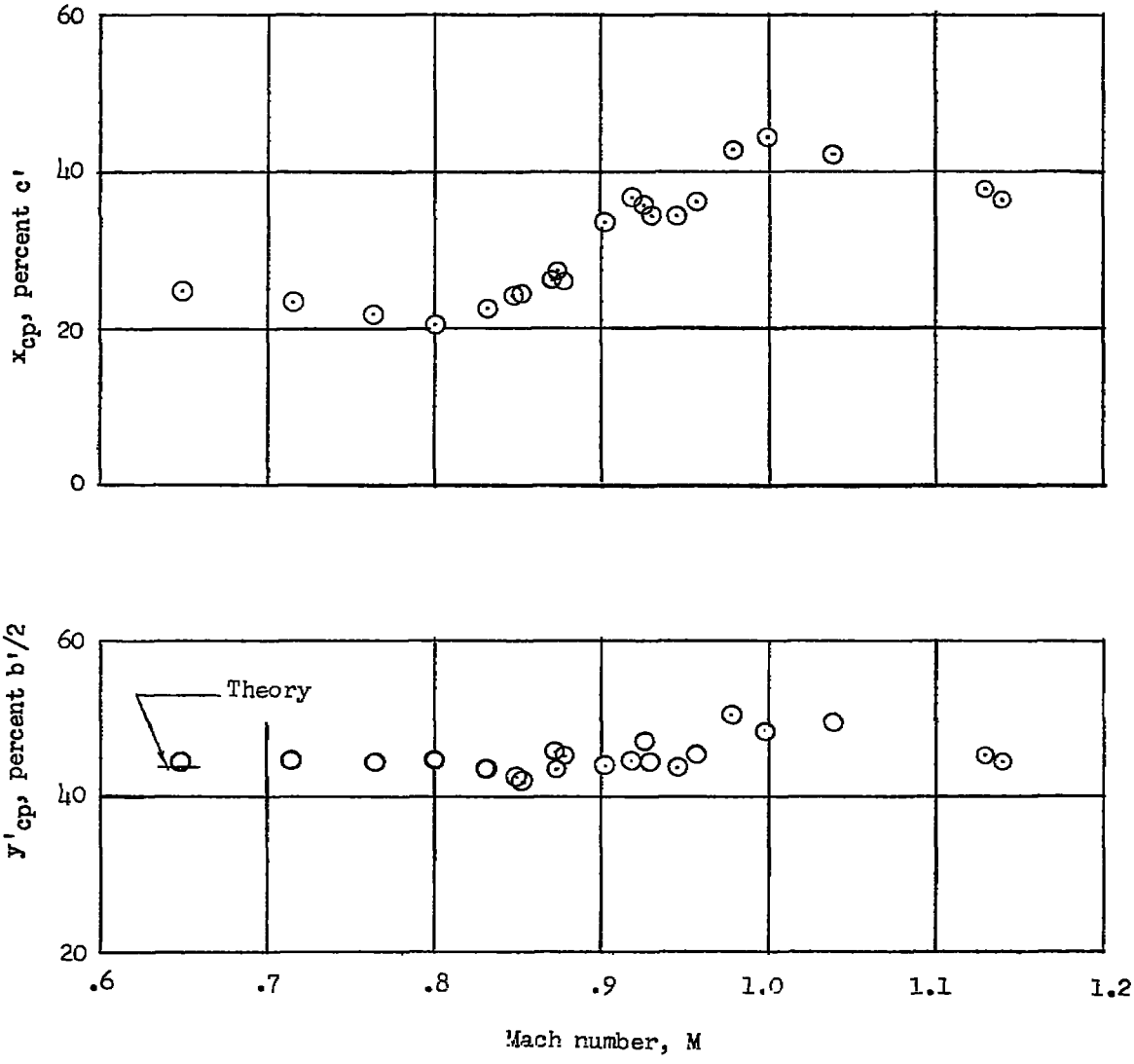

Figure 12.- Variation of spanwise and chordwise centers of pressure of the wing panel with Mach number.

[redacted]